LAWRENCE
LIVERMORE
NATIONAL
LABORATORY

LLNL-JRNL-668475

Atomic origin of 3d94f1 configuration in La3+ solids

S. W. Yu, M. H. Carpenter, F. Ponce, S. Friedrich, J. S. Lee, D. Aberg

March 12, 2015

Physical Review Letter

Disclaimer

This document was prepared as an account of work sponsored by an agency of the United States government. Neither the United States government nor Lawrence Livermore National Security, LLC, nor any of their employees makes any warranty, expressed or implied, or assumes any legal liability or responsibility for the accuracy, completeness, or usefulness of any information, apparatus, product, or process disclosed, or represents that its use would not infringe privately owned rights. Reference herein to any specific commercial product, process, or service by trade name, trademark, manufacturer, or otherwise does not necessarily constitute or imply its endorsement, recommendation, or favoring by the United States government or Lawrence Livermore National Security, LLC. The views and opinions of authors expressed herein do not necessarily state or reflect those of the United States government or Lawrence Livermore National Security, LLC, and shall not be used for advertising or product endorsement purposes.

Atomic origin of $3d^9 4f^1$ configuration in La^{3+} solids

S.-W. Yu,[1,*] M. H. Carpenter,[1,2] F. Ponce,[1,2] S. Friedrich,[1] J.-S. Lee,[3] and D. Åberg[1]

[1] *Lawrence Livermore National Laboratory, Livermore, CA, USA*

[2] *University of California at Davis, Davis, CA, USA*

[3] *Stanford Synchrotron Radiation Lightsource, Menlo Park, CA, USA*

Abstract

We have studied the excited electronic structure of $LaBr_3$(Ce) scintillator by soft x-ray spectroscopy. The La $M_{4,5}$-edges x-ray absorption spectrum from $LaBr_3$(Ce) is compared with the ones from other La^{3+} solids (La_2O_3, LaF_3 and La metal). From this comparison, it is turned out that the La absorption spectra from all the La^{3+} solids considered here appear at the almost same energy, even though the corresponding energies of the $3d$ core holes are very different. As a result, it is argued that the atomic nature of the $3d^9 4f^1$ configuration is maintained via the $4f^1$ state, which screens the $3d$ core holes differently from one La^{3+} solid to other one.

* Corresponding Author: yu21@llnl.gov

Recently invented $LaBr_3$(Ce) scintillator [1], cerium doped $LaBr_3$ crystal, motivated not only to develop new scintillator by co-doping [2], but also to understand its fundamental electronic structure [3–6]. From the electronic structure's point of view, a physical prerequisite to be a good scintillator for $LaBr_3$(Ce) is that the $4f^1$ and $5d^0$ states of trivalent Ce activator have to be located in the fundamental band gap of host $LaBr_3$ crystal, so that holes and electrons moving through the valence and conduction bands of host can be captured by the $4f^1$ and $5d^0$ states, respectively [5]. However, under normal operational condition of $LaBr_3$(Ce) scintillator, incoming γ-rays disturb the electronic structures of host and activator significantly. For example, when γ-rays are absorbed in $LaBr_3$(Ce), γ-rays can remove electrons from every core levels, i.e., they create holes in every core levels. When a core hole in the $3d$ core level of Ce activator is created by the incoming γ-rays, the energy of $4f^1$ state is changed by the attractive Coulomb potential of the $3d$ core hole, meaning that the energetic position of $4f^1$ state with respect to the top of the valence band is changed [7]. Such change can influence on the performance of the scintillator [7].

Another example is La $3d$ core hole of host $LaBr_3$. When a La $3d$ core hole is created, the core hole pulls down the empty La $4f^0$ state near the valence band of host [8, 9]. Then, in order to screen the $3d$ core hole, the empty La $4f^0$ state interacts with the valence band via a charge transfer from the valence band, resulting in the $4f^1\underline{v}$ state, where $\underline{v}$ is a hole in the valence band. To our best knowledge, it is still open question how the $4f^1\underline{v}$ state of La interacts with the $4f^1$ of Ce activator in the excited state, and furthermore whether the interaction can influence on the performance of the scintillator. Understanding the excited electronic structure of the scintillator in the presence of core holes is important to answer to those open questions.

X-ray photoelectron spectroscopy (XPS) and x-ray absorption spectroscopy (XAS) are very suitable spectroscopic methods to study the excited electronic structures in the presence of core holes [8–10]. The essential difference between XPS and XAS in La^{3+} solids can be understood in the following way. In the final state of $3d$ XPS, a $3d$ core electron is excited into the continuum state and a $3d$ core hole is created. Then, in order to screen the core hole, the system rearranges in such a way that the La empty $4f$ state pulled down by the core hole receives an electron from the valence band. As a result, the $3d$ XPS spectra show not only the main peak ($3d^9 4f^0$), but also the satellite ($3d^9 4f^1\underline{v}$), which strongly depend on La^{3+} solids [11–13]. In $3d$ XAS, however, a $3d$ electron is excited into the empty $4f$ state

and the XAS process can be described by $3d^{10}4f^0 \rightarrow 3d^9 4f^1$, in which $4f^1$ electron screens the $3d$ core hole. In contrast to the $3d$ XPS, all the $3d$ XAS spectra appear at the same energy and are identical, independently on La^{3+} solids [14–17]. The physical reason for the behaviour of the $3d$ XAS spectra is known to be due to atomic character of the $3d^9 4f^1$ configuration. But there is no clear picture how the $3d^9 4f^1$ configuration keeps the atomic nature in different solids, because the energy of the $3d$ core hole and the energy of $4f^1$ state change from one solid to other one.

The aim of this letter is to provide a clear picture how the $3d^9 4f^1$ configuration maintains its atomic nature in different La^{3+} solids. We have chosen four La^{3+} solids: three insulating compounds ($LaBr_3$(Ce), LaF_3, and La_2O_3), and La metal. For all four materials, the binding energies of La $3d_{5/2}$ (M_5) core levels and the energies of La $4f^0$ states are plotted with respect to a common energy level: the top of the valence band for three insulating La solids and the Fermi level for La metal. From this plot, it is turned out that the binding energy of La $3d_{5/2}$ (M_5) core level and the energy of La $4f^0$ state in the ground state depend on four La^{3+} solids. Then, based on the energies from the $3d_{5/2}$ (M_5) XAS spectra, the energies of La $4f^1$ state are located for four La^{3+} solids. From this layout, it is demonstrated that the energies of the $3d$ core holes change from one material to other one. But the energies of the $4f^1$ states also change correspondingly, so that the distance in energy between the $3d$ core hole and the $4f^1$ state is kept the constant, resulting in that the $3d^9 4f^1$ configuration keeps its the atomic character even in solids.

The $M_{4,5}$-edges XAS measurements from $LaBr_3$(Ce) and La_2O_3 were performed at beam line 8-2 of the Stanford Synchrotron Radiation Lightsource (SSRL) at SLAC National Accelerator Laboratory [18]. The XAS spectra were accumulated by the total electron yield (TEY) and normalized to the beam flux (I_0) measured by a gold mesh. The $M_{\alpha,\beta}$-edges XES measurements with an electron beam of 3 keV were performed at the Lawrence Livermore National Laboratory [19]. The commercially available $LaBr_3$(5%Ce) scintillator (Brillance 380) was purchased from SAINT-GOBAIN. Due to very hygroscopic nature of $LaBr_3$(Ce), it was delivered encapsulated in aluminium housing. In glove box of argon atmosphere, the housing was removed, and $LaBr_3$(Ce) crystal was broken into small pieces of about 0.5 mm in diameter, to minimize the charging effect [7]. Then, $LaBr_3$(Ce) was introduced into the vacuum chamber for the measurements without exposing to the air. No charging effect was observed in the XAS measurements. The other commercially available reference samples

of La_2O_3 powder (3N purity), CeO_2 powder (3N purity), CeF_3 powder (3N purity) were purchased from Alfa Aesar and ESPI Metals. They were handled in glove box just like $LaBr_3$(Ce).

The upper panel of Figure 1 presents $M_{4,5}$-edges XAS spectrum from La and Ce of $LaBr_3$(Ce). The La $M_{4,5}$-edges XAS spectrum consists of the two single peaks corresponding to $M_5(3d_{5/2})$ and $M_4(3d_{3/2})$ states split by the spin-orbit interaction, respectively, with a very weak structure (A) at the lower energy side of M_5 peak. The La $M_{4,5}$-edges XAS spectrum from La_2O_3 is also shown, which is identical to the one of $LaBr_3$(Ce), except for a little bit shifting ($\sim$0.2 eV) to the lower energy side. The Ce $M_{4,5}$-edges XAS spectrum is also visible, but very weak compared to that of La due to the low concentration of the Ce activator. We will discuss further about the Ce $M_{4,5}$-edges XAS spectrum at the later part of this paper.

The La $M_{4,5}$-edges XAS spectrum can be understood by the symmetry of the atomic multiplets [20]. In case of La^{3+}, the $3d \rightarrow 4f$ x-ray absorption process excites a $3d$ core electron to the empty $4f$ state ($3d^{10}4f^0 \rightarrow 3d^9 4f^1$). In the ground state, the $3d^{10}4f^0$ configuration has only completely filled $3d^{10}$ and empty $4f^0$ states. Therefore, it has $^1S_0$ symmetry, indicating that all the quantum numbers (S, L, and J) are zero. In the final state, the $3d^9 4f^1$ configuration has a $3d$ core hole and a $4f$ electron. Under the two particles interaction, there are 20 possible symmetries in the final state. However, due to the dipole selection rule ($\Delta J = 1$), the only allowed symmetries in the final state are $^3P_1$, $^3D_1$, and $^1P_1$ [16, 20]. In the upper panel of Figure 1, the peak A corresponds to $^3P_1$ while the La M_5 and M_4 peaks correspond to $^3D_1$ and $^1P_1$, respectively. Our La $M_{4,5}$-edges XAS spectrum from $LaBr_3$(Ce) is identical with other previous experimental results on the trivalent La^{3+} [14, 15].

The La and Ce $M_{\alpha,\beta}$-edges XES spectra from $LaBr_3$(Ce) are shown in the lower panel of Figure 1. Similar to the $M_{4,5}$-edges XAS spectra, the $M_{\alpha,\beta}$-edges XES spectrum from La shows the two peaks corresponding to the spin-orbit splitting M_α ($3d_{5/2}$) and M_β ($3d_{3/2}$) states, respectively. In addition, a satellite peak (S) at the lower energy side of La M_α peak is observed. The intensity of Ce $M_{\alpha,\beta}$-edges XES part is very weak compared to the one of La as expected. The La $M_{\alpha,\beta}$-edges XES spectrum from La_2O_3 is identical to the one of $LaBr_3$(Ce).

The La $M_{\alpha,\beta}$-edges XES spectrum can be ascribed to the emission process of $3d^9 4f^1 \rightarrow 3d^{10}4f^0$ [10, 21, 22]. Since the La has $4f^0$ configuration in the ground state, an electron

has to be supplied into the empty $4f$ state in the presence of a $3d$ core hole to reach the initial state $3d^9 4f^1$ configuration. The $3d^9 4f^1$ configuration, which is the final state of La $M_{4,5}$-edges XAS ($3d^{10}4f^0 \rightarrow 3d^9 4f^1$), can be created with an electron beam of 3 keV in the following ways. First, it can be reached by a direct excitation from a $3d$ core electron to the empty $4f$ state because under the electron bombardment the $3d$ core electron can absorb any amount of the energy from the incident electron, in contrast to the case where a photon beam is used [21, 22]. For example, if a photon beam of 3 keV is used, the $3d$ core electron must absorb the entire photon energy of 3 keV, and is excited into the continuum (in other words, leaves the La atom as photoelectron) and therefore there is no possibility that the $3d$ core electron can be excited into the empty $4f$ state. Second, an incident electron can be trapped into the empty $4f$ state under the presence of the $3d$ core hole [22].

As shown for the cases of $LaBr_3$(Ce) and La_2O_3 in Figure 1, it is well known that La $M_{4,5}$-edges XAS and $M_{\alpha,\beta}$-edges XES spectra appear at the same energy [10, 23]. Furthermore, La $M_{4,5}$-edges XAS spectra from $LaBr_3$(Ce) and La_2O_3 appear at the same energy of about 835.0 eV, even though the corresponding La $3d$ XPS spectra appear at the very different binding energies [11, 13, 24]. In order to understand it quantitatively, the electronic structures of $LaBr_3$(Ce) [11, 25, 26] and La_2O_3 [24, 27, 28] are summarized in Figure 2. Even though we have not performed XAS measurements on LaF_3 and La metal within this paper, we added their electronic structures based on the experimental data from other literatures [10–12, 25, 26, 29–32]. In Figure 2, for three insulating materials (LaF_3, La_2O_3, $LaBr_3$(Ce)), the top of the valence band is defined as the energy zero point, and for La metal, the Fermi level is the energy zero point.

In case of $LaBr_3$(Ce), the La $4f^0$ lies at 7.7 eV in the ground state [26] and the binding energy of La $3d_{5/2}$ core level is −832.8 eV [11, 25]. Therefore, La M_5 XAS spectrum is expected to appear at the energy of 840.5 eV (832.8 eV + 7.7 eV = 840.5 eV). However, in reality, it is observed at the energy of 835.1 eV. This indicates that La $4f^0$ state at 7.7 eV in the ground is lowered to $4f^1$ state at 2.3 eV in the final state after the $3d^{10}4f^0 \rightarrow 3d^9 4f^1$ process. Similarly, for La_2O_3, the La $4f^0$ lies at 11.1 eV in the ground state [28] and the binding energy of La $3d_{5/2}$ core level is −831.7 eV [24]. Under this condition, La M_5-edge XAS spectrum is supposed to appear at the energy of 842.8 eV (831.7 eV + 11.1 eV = 842.8 eV). But, it is observed at the energy of 834.9 eV, meaning that La $4f^0$ state at 11.1 eV in the ground state is changed to $4f^1$ state at 3.2 eV in the final state of XAS.

The identical behaviour is observed for LaF_3, in which the La $4f^0$ lies at 12.4 eV in the ground state [29] and the binding energy of La $3d_{5/2}$ core level is at -830.6 eV [11, 25]. In this case, La M_5-edge XAS is expected at the energy of 843.0 eV (830.6 eV + 12.4 eV = 843.0 eV). However, it is observed at the energy of 834.5 eV [32], again indicating that La $4f^0$ state at 12.4 eV in the ground state is lowered to $4f^1$ state at 3.9 eV in the final state of XAS. We notice that La M_5-edge XAS energy (834.5 eV) of LaF_3 is lower by $\sim$0.5 eV than the ones of $\sim$835 eV for La_2O_3 and $LaBr_3$(Ce). This difference could be caused by the different calibrations for different experiments, because it is known that La XAS spectra from all the La^{3+} compounds appear at the same energy [10, 15, 17, 21]. Therefore, if we assume La M_5-edge XAS energy of LaF_3 to be 835.0 eV, then the $4f^1$ would be at 4.4 eV.

For the La metal, the binding energy of La $3d_{5/2}$ is about -835.8 eV and the $4f^0$ state in the ground state is at 5.5 eV with respect to the Fermi level [10, 30, 31]. In this case, La M_5-edge XAS is expected at the energy of 841.3 eV (835.8 eV + 5.5 eV = 841.3 eV). However, it is observed at the energy of $\sim$834.6 eV [14, 23, 33]. In the case of La metal, the XAS energy is smaller than the binding energy of La $3d_{5/2}$ by 1.2 eV, meaning that La $4f^0$ state at 5.5 eV in the ground state is lowered to $4f^1$ state at -1.2 eV below the Fermi level in the final state of XAS.

As it is clear from Figure 2, the La $3d_{5/2}$ binding energies and the $4f^0$ energies in the ground state, and the $4f^1$ energies in the final state of XAS depend on the La^{3+} solids (three insulating La compounds and La metal). However, the La M_5 XAS energies are identical for all the insulating La compounds and La metal considered within this work. The physical origin for the behaviour can be understand in the following way: when the energy of the La $3d_{5/2}$ core hole changes from one La solid to another one, the energy of the $4f^1$ state associated with $3d^9 4f^1$ configuration also changes in such a way that the energy distance between the $3d_{5/2}$ core hole and the $4f^1$ state is kept the constant. In other words, the $4f^1$ electron screens the $3d_{5/2}$ core hole differently from one La solid to another one, in order to maintain the strong atomic nature of $3d^9 4f^1$ configuration even in solids.

The energies of $4f^1$ states determined by La M_5-edge XAS spectra in Figure 2 can be estimated by another independent approach, so-called Z+1 approximation. Creation of a $3d$ core hole can be approximated by adding a proton to the nucleus [8, 9]. This means that the $3d^9 4f^1$ configurations of LaF_3, La_2O_3, $LaBr_3$, and La metal correspond to the $4f^1$ configurations of CeF_3, Ce_2O_3, $CeBr_3$, and Ce metal. In fact, the valence band XPS spectra

from CeF_3, Ce_2O_3, $CeBr_3$, and Ce metal show that the energies of $4f^1$ states lie ∼4.8 eV for CeF_3 [34], ∼3.6 eV for Ce_2O_3 [35], ∼2.8 eV for $CeBr_3$ [34], above the center of the valence band [36]. For Ce metal it is at −1.8 eV below the Fermi level [8, 9].

The satellite peak S shown in La M_α-edge XES spectrum from $LaBr_3$(Ce) (Figure 1) provides an additional evidence for the $4f^1$ position [10, 21]. The peak S is initially known due to the transition of $5p_{3/2} \rightarrow 3d_{5/2}$ [10, 21]. Then, since the binding energy difference between $3d_{5/2}$ and $5p_{3/2}$ is 816.5 eV (832.8 eV−16.3 eV=816.5 eV), the peak S is supposed to appear at the energy of 816.5 eV. However, it is observed at the energy of 812.0 eV in Figure 1, and the $4f^1$ state is responsible for the smaller energy [10]. The $5p$ electrons are repelled by the $4f^1$ electron as a spectator, and the energy of the $5p_{3/2} \rightarrow 3d_{5/2}$ transition is smaller. Therefore, the peak S is assigned to the transition of $5p_{3/2}4f^1 \rightarrow 3d_{5/2}4f^1$ [10, 21].

Finally, in the right upper side of Figure 1, the Ce $M_{4,5}$-edges XAS spectrum from $LaBr_3$(Ce) is enlarged and compared with CeF_3 (Ce^{3+}) and CeO_2 (Ce^{4+}). Clearly, Ce $M_{4,5}$-edges XAS spectrum shows the multiplets due to the $3d^4 4f^2$ and overlaps with the one from CeF_3 (Ce^{3+}). Therefore, it is concluded that the Ce activator of $LaBr_3$(Ce) scintillator is in trivalent Ce^{3+}.

In conclusions, we measured the La $M_{4,5}$-edges XAS and $M_{\alpha,\beta}$-edges XES from $LaBr_3$(Ce) and La_2O_3. We also used the La $M_{4,5}$-edges XAS spectra of LaF_3 and La metal from the literatures for our discussion. It turned out that all XAS and XES spectra appear at the identical energy of about 835 eV, due to the strong atomic nature of the $3d^9 4f^1$ configuration. It is argued that the $4f^1$ state screens the $3d$ core hole differently from one La^{3+} solid to other one, in order to maintain the atomic nature of the $3d^9 4f^1$ configuration even in solids.

Lawrence Livermore National Laboratory is operated by Lawrence Livermore National Security, LLC, for the U.S. Department of Energy, National Nuclear Security Administration under Contract DE-AC52-07NA27344. This work was funded by the Laboratory Directed Research and Development Program at LLNL under project tracking code LDRD 13-ERD-038. SSRL, a Directorate of SLAC and an Office of Science User Facility operated for the US DOE Office of Science by Stanford University. J.S.L acknowledges partial support by the Department of Energy, Office of Basic Energy Sciences, Materials Sciences and Engineering

Division, under contract DE-AC02-76SF00515.

---

[1] E. V. D. van Loef, P. Dorenbos, C. W. E. van Eijk, K. Krämer, and H. U. Güdel, Appl. Phys. Lett. **79**, 1573 (2001).

[2] M. S. Alekhin, J. T. M. de Haas, I. V. Khodyuk, K. W. Krämer, P. R. Menge, V. Ouspenski, and P. Dorenbos, Appl. Phys. Lett. **102**, 161915 (2013).

[3] G. Bizarri and P. Dorenbos, Phys. Rev. B **75**, 184302 (2007).

[4] D. Åberg, B. Sadigh, and P. Erhart, Phys. Rev. B **85**, 125134 (2012).

[5] A. Canning, A. Chaudhry, R. Boutchko, and N. Grønbech-Jensen, Phys. Rev. B **83**, 125115 (2011).

[6] D. J. Singh, Phys. Rev. B **82**, 155145 (2010).

[7] S.-W. Yu, M. H. Carpenter, F. Ponce, S. Friedrich, J.-S. Lee, P. Olalde-Velasco, W. L. Yang, and D. Åberg, submitted to Journal of Physics: Condended Matter (2015).

[8] G. Crecelius, G. K. Wertheim, and D. N. E. Buchanan, Phys. Rev. B **18**, 6519 (1978).

[9] G. K. Wertheim and M. Campagna, Solid State Commun. **26**, 553 (1978).

[10] P. Motais, E. Belin, and C. Bonnelle, Phys. Rev. B **30**, 4399 (1984).

[11] S. Suzuki, T. Ishii, and T. Sagawa, J. Phys. Soc. Jpn. **37**, 1334 (1974).

[12] S.-J. Oh, G.-H. Kim, G. A. Sawatzky and H. T. Jonkman, Phys. Rev. B **37**, 6145 (1988).

[13] A. J. Signorelli and R. G. Hayes, Phys. Rev. B **8**, 81 (1973).

[14] B. T. Thole, G. van der Laan, J. C. Fuggle, G. A. Sawatzky, R. C. Karnatak, and J.-M. Esteva, Phys. Rev. B **32**, 5107 (1985).

[15] G. Kaindl, G. Kalkowski, W. D. Brewer, B. Perscheid, and F. Holtzberg, J. Appl. Phys. **55**, 1910 (1984).

[16] C. Bonnelle, R. C. Karnatak, and J. Sugar, Phys. Rev. A **9**, 1920 (1974).

[17] S. Suzuki, T. Ishii, and T. Sagawa, J. Phys. Soc. Jpn. **38**, 156 (1975).

[18] J.R.I. Lee, T.Y.-J. Han, T.M. Willey, D. Wang, R.W. Meulenberg, J. Nilsson, P.M. Dove, L.J. Terminello, T. van Buuren, J.J. De Yoreo, Journal of the American Chemical Society **129**, 10370 (2007).

[19] S.-W. Yu, J. G. Tobin, and B. W. Chung, Rev. Sci. Instrum. **82**, 093903 (2011).

[20] F. de Groot and A. Kotani, *Core Level Spectroscopy of Solids*, CRC Press, Boca Raton,

Florida, 2008.

[21] M. Okusawa, K. Ichikawa, O. Aita, and K. Tsutsumi, Phys. Rev. B **35**, 478 (1987).

[22] K. Ichikawa, A. Nisawa, and K. Tsutsumi, Phys. Rev. B **34**, 6690 (1986).

[23] D. W. Fischer and W. L. Baun, J. Appl. Phys. **38**, 4830 (1967).

[24] M. F. Sunding, K. Hadidi, S. Diplas, O. M. Lvvik, T. E. Norby, A. E. Gunns, J. Electron Spectrosc. Relat. Phenom. **184**, 399 (2011).

[25] S. Sato, J. Phys. Soc. Jpn. **41**, 913 (1976).

[26] E. Rogers, P. Dorenbos, and E. van der Kolk, New Journal of Physics **13**, 093038 (2011).

[27] A. V. Prokofiev, A. I. Shelykh, and B. T. Melekh, J. Alloys Comp., **242**, 41 (1996).

[28] W.-D. Schneider, B. Delley, E. Wuilloud, J.-M. Imer, and Y. Baer, Phys. Rev. B **32**, 6819 (1985).

[29] K.-H. Park and S.-J. Oh, Phys. Rev. B **48**, 14833 (1993).

[30] J. K. Lang, Y. Baer and P. A. Cox, J. Phys. F: Metal Phys. **11**, 121 (1981).

[31] J. Kanski, P. O. Nilsson and I. Curelaru, J. Phys. F: Metal Phys. **6**, 1073 (1976).

[32] G. Van Der Laan and B. T. Thole, J. Electron Spectrosc. Relat. Phenom. **46**, 123 (1988).

[33] In reference [14], the M_5 XAS energy is 834.2 eV. This difference could be caused by the different calibrations for different experiments.

[34] A. Fujimori, T. Miyahara, T. Koide, T. Shidara, H. Kato, H. Fukutani, and S. Sato, Phys. Rev. B **38**, 7789 (1988).

[35] D. R. Mullins, S. H. Overbury, and D. R. Huntley, Surf. Sci. **409**, 307 (1998).

[36] Due to the ambiguity to determine the top of the valence band, the center of the valence band is used as the reference points for CeF_3, Ce_2O_3, $CeBr_3$.

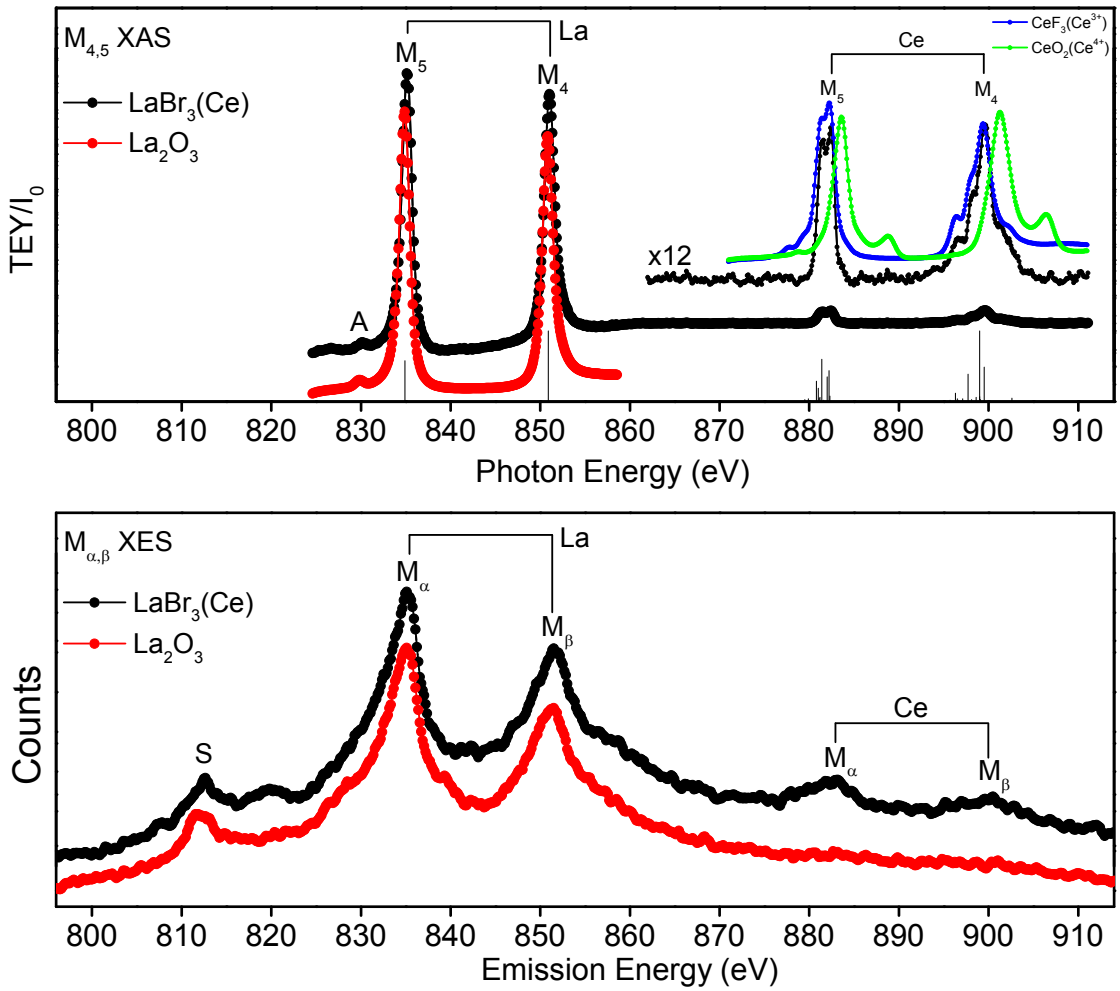

FIG. 1. (Color online) Upper panel: $M_{4,5}$-edges XAS spectra from $LaBr_3(Ce)$ and a reference sample La_2O_3. Due to the low concentration of cerium, the cerium signal is very weak. The vertical thin lines represent the theoretical multiplet splittings due to the $3d^9 4f^1$ configuration for La^{3+} and the $3d^9 4f^2$ configuration for Ce^{3+}, respectively. In the right upper side, Ce $M_{4,5}$-edges XAS spectrum from $LaBr_3(Ce)$ is enlarged and compared with CeF_3 (Ce^{3+}) and CeO_2 (Ce^{4+}). Lower panel: $M_{\alpha,\beta}$ XES spectra from $LaBr_3(Ce)$ and La_2O_3. An electron beam of E=3 keV is used to create the $3d$ core holes. In addition to the main $M_{\alpha,\beta}$ peaks, a satellite peak (S) is observed for both $LaBr_3(Ce)$ and La_2O_3. For La, $M_{\alpha,\beta}$ XES spectrum is due to the transition of $3d^9 4f^1 \rightarrow 3d^{10} 4f^0$ while the satellite (S) is due to the transition of $5p_{3/2} 4f^1 \rightarrow 3d_{5/2} 4f^1$.

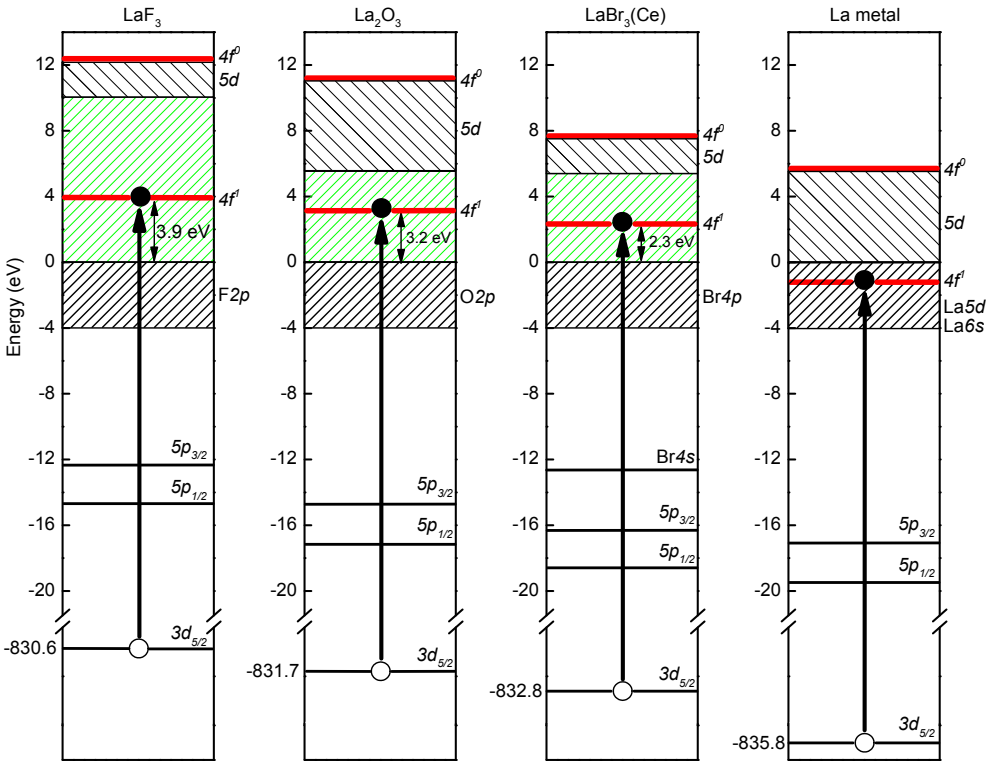

FIG. 2. (Color online) Energy level diagrams for LaF_3, La_2O_3, $LaBr_3$(Ce) and La metal. For three insulating materials (LaF_3, La_2O_3, $LaBr_3$(Ce)), the top of the valence band is defined as the energy zero point, while for La metal the Fermi level is the energy zero point. The band gaps for three insulating materials are marked by the green lines. For all the four materials, the binding energies of La $3d_{5/2}$ core levels are determined from the main lines ($3d^9 4f^0$) of $3d$ XPS spectra. The error ± 0.3 eV should be added for all the energy levels determined because of the uncertainty in determination of the energy levels from various experiments. For LaF_3, the fundamental band gap is 10 eV [26]. La $4f^0$ lies at 12.4 eV [29] and La $3d_{5/2}$ is at -830.6 eV [11, 25]. In the XAS final state, La $4f^1$ is lowered to 3.9 eV, and therefore, M_5 XAS spectrum appears at the energy of 834.5 eV [32]. For La_2O_3, the fundamental band gap is 5.5 eV [27]. La $4f^0$ lies at 11.1 eV [28] and La $3d_{5/2}$ is at -831.7 eV [24]. In the XAS final state, La $4f^1$ is lowered to 3.2 eV, and therefore, M_5 XAS spectrum appears at the energy of 834.9 eV (this work). For $LaBr_3$(Ce), the fundamental band gap is 5.4 eV [25]. La $4f^0$ lies at 7.7 eV [26] and La $3d_{5/2}$ is at -832.8 eV [11, 25]. In the XAS final state, La $4f^1$ is lowered to 2.3 eV, and therefore, M_5 XAS spectrum appears at the energy of 835.1 eV (this work). For La metal, La $4f^0$ lies at 5.5 eV [30] and La $3d_{5/2}$ is at -835.8 eV [31]. In the XAS final state, La $4f^1$ is lowered to -1.2 eV, i.e., below the Fermi level, and therefore, M_5 XAS spectrum appears at the energy of 834.6 eV [14, 23].